Editors' Suggestion

Probing the Shell Effects on Fission: The New Superheavy Nucleus ^{257}Sg

P. Mosat,[1,*] J. Khuyagbaatar,[1,†] J. Ballof,[1] R. A. Cantemir,[1] D. Dietzel,[2] Ch. E. Düllmann,[1,2,3] K. Hermainski,[2] F. P. Heßberger,[1] E. Jäger,[1] B. Kindler,[1] J. Krier,[1] N. Kurz,[1] B. Lommel,[1] S. Löchner,[1] M. Maiti,[4] T. K. Sato,[5] B. Schausten,[1] J. Uusitalo,[6] P. Wieczorek,[1] and A. Yakushev[1]

[1]*GSI Helmholtzzentrum für Schwerionenforschung, 64291, Darmstadt, Germany*
[2]*Johannes Gutenberg-Universität Mainz, 55099 Mainz, Germany*
[3]*Helmholtz Institute Mainz, 55099 Mainz, Germany*
[4]*Indian Institute of Technology, Roorkee, Roorkee 247667, India*
[5]*Advanced Science Research Center, Japan Atomic Energy Agency, Tokai, Ibaraki 319-1195, Japan*
[6]*University of Jyväskylä, 40351 Jyväskylä, Finland*

(Received 12 February 2025; revised 10 April 2025; accepted 7 May 2025; published 11 June 2025)

Decay properties of the neutron-deficient Sg isotopes were studied at the gas-filled recoil separator TASCA at GSI, Darmstadt by using the ^{52}Cr + ^{206,208}Pb reactions. We report on the discovery of the new isotope ^{257}Sg. Its ground state, tentatively assigned to have $9/2^-[734]$ configuration, was observed to decay by both spontaneous fission and α-particle emission with a half-life of $12.6^{+3.7}_{-2.3}$ ms. The alpha decay from this high-spin state was followed by fission of ^{253}Rf after 11 μs. In ^{259}Sg, we observed strong evidence for the occurrence of a K-isomeric state for the first time in superheavy nuclei with 106 protons. The current experimental findings, discussed within the experimental systematics and theory, indicate that hitherto unseen features of the shell effect on the fission process may be found in the neutron-deficient superheavy nuclei.

DOI: 10.1103/s7hr-y7zq

The fission of a heavy nucleus, driven by the repulsive Coulomb force, is a main destructive process for the many-nucleon systems bound by the attractive nuclear force. Quantum shell effects counteract the fission process and prevent the instant disruption of nuclei with $Z > 103$, which would otherwise fission on very short (i.e., $< 10^{-14}$ s) timescale and are referred to as superheavy [1,2]. These effects prolong the spontaneous fission half-life (T_{SF}), with the effect being stronger when an energy gap between nucleon orbitals is large. This is well visible in the measured T_{SF} of the even-even nuclei [3], where all nucleons are paired, resulting in the total spin $J = 0$, and thus, its projection onto the symmetry axis K is 0. This experimental systematics represents the fission landscape of the heaviest nuclei.

In the case of odd-A or odd-odd nuclei, fission is additionally retarded due to the nonzero total spin, i.e., $K > 0$. Such single-particle effects lead to T_{SF} that are longer than those of the adjacent even-even nuclei [3,4]. Theoretically this was explained to be caused by the conservation of quantum numbers (e.g., K) during the nuclear-shape evolution from the ground state towards the saddle point [5,6]. The effect of the single-particle configuration on fission, however, is not yet fully understood while for even-even nuclei a theoretical description is better established even though it is still not satisfactory [7].

In this regard, recently acquired data on fission of neutron-deficient odd-A [8–10] and odd-odd [11] nuclei call for a revision of the single-particle effect on fission. Among these, of special interest are the data on ^{253}Rf [9]. The experimental data obtained in Ref. [9] led to the conclusion that the two fission activities in ^{253}Rf with half-lives of 9.9 ms and 58 μs originate from ($K = 1/2$) and ($K = 7/2$) states, respectively. This finding, which is in contradiction with the experimental systematics and with the commonly accepted concept for a relation between the fission hindrance and the K quantum number [3,5,6,8,12,13], needs to be confirmed. A complementary approach is to investigate fission from a state in ^{253}Rf that is selectively populated via α decay from the hitherto unknown ^{257}Sg.

On the other hand, the experimental data on K-isomeric states in Fm-Ds isotopes [14–18] show that fission of such states is largely hindered, which supports an impact of the K quantum number on fission. This was most prominently observed in the recently discovered ^{252}Rf [18], where a high-K state lives about 200 times longer than its 60-ns ground state. This confirmed the anticipated approach for

*Contact author: P.Mosat@gsi.de
†Contact author: J.Khuyagbaatar@gsi.de

Published by the American Physical Society under the terms of the Creative Commons Attribution 4.0 International license. Further distribution of this work must maintain attribution to the author(s) and the published article's title, journal citation, and DOI.

the synthesis of the extremely short-lived nuclei in the vicinity of the isotopic border (where the nucleus' T_{SF} is $< 10^{-14}$ s) via long-lived K-isomeric states [19–24]. The next step is to explore the isotopic border in Sg isotopes, where, however, no K-isomeric state was reported yet.

In this Letter, we report on the discovery of the new isotope ^{257}Sg, on the study of fission of its α-decay daughter ^{253}Rf, and on the evidence for a K-isomeric state in ^{259}Sg.

The experiment was carried out at the gas-filled recoil separator TASCA [25] at GSI Helmholtzzentrum für Schwerionenforschung, Darmstadt, Germany. A $^{52}Cr^{14+}$ beam, produced from a Penning-ion-gauge ion source, was accelerated by the Universal Linear Accelerator UNILAC to an energy of 257.5 MeV, delivered in 5-ms-long pulses with 50-Hz repetition rate. The four-segment target wheel was rotating synchronously with the beam-pulse structure [26]. Irradiation of a particular segment by a beam pulse was tracked by two binary signals. The average beam intensity on the target was $\approx 7 \times 10^{12}$ particles per second.

First, we measured the known $^{52}Cr + ^{208}Pb$ reaction [27] to find the optimal beam energy (E_b) for the $1n$ evaporation channel. This was performed with four ^{208}PbS targets (Run 1) and later with two ^{208}PbS (Run 2) target segments. The two other segments in Run 2 were ^{206}PbS. Finally, all targets were ^{206}PbS (Run 3). The average thickness of targets was ≈ 0.75 mg/cm^2. The beam energies in the middle of the targets were $E_b = 252.4$ (Run 1) and 250.8 MeV (Run 2) for the $^{52}Cr + ^{208}Pb$ reaction [Fig. 1(a)]. Three beam energies of $E_b = 252.4$ (Run 2), 251.6 (Run 3), and 249.0 MeV (Run 3) were used for the $^{52}Cr + ^{206}Pb$ reaction [Fig. 1(b)].

The evaporation residues (ERs) were separated from the primary beam and products of other reactions by the gas-filled recoil separator TASCA, operated with 0.8 mbar helium and set to a magnetic rigidity ($B\rho$) of 2.14 Tm [28,29]. The efficiency of TASCA to guide ERs to the focal plane was estimated to be 60% [28,30,31]. At the focal plane after passing through 3.6-μm-thick Mylar foil, ERs were implanted into a double-sided silicon detector with 144 vertical (X) and 48 horizontal (Y) strips on the front and back sides, respectively. Signals from the implantation and subsequent decays were acquired from both X and Y strips with preamplification ranges up to about 20 and 200 MeV, respectively. The data acquisition system was triggered by X and/or Y strip signals. In the present experiment, only 118 X-strips were read out. The energy resolution (FWHM) was about 50 keV for 5.8-MeV α particles. All signals were digitized by 100-MHz-sampling 14-bit FEBEX4 analog-to-digital converters [32,33] and were stored in 80-μs-long traces [34]. Two-bit signals from the target-rotation control system providing tagging of the irradiated target segment were read out for each event trigger; the rate was ≈60 Hz.

Decays of Sg isotopes were searched for via ER–FI ($\Delta t < 1$ s), ER–α ($\Delta t < 10$ s), and α–FI ($\Delta t < 10$ s) correlations requiring the same X and Y strips. Data rates for ER-like (beam-on) and α-like (beam-off) events with energies of 10–25 and 8–10 MeV, respectively, were ≈12 Hz and ≈0.01 Hz. Beam-on and beam-off events in the ranges of (90–200) MeV and (60–200) MeV, respectively, with counting rates of ≈0.01 Hz were considered to be fission signals (FI). Once a correlation was found, an event-by-event analysis was performed for each candidate to reconstruct the full Sg decay sequence.

In the $^{52}Cr + ^{208}Pb$ reaction (Runs 1 and 2), one and four chains representing ER–FI and ER–α–α/FI sequences, respectively, were observed and attributed to ^{258}Sg and ^{259}Sg. In Fig. 1(c), the correlation times Δt of these Sg events are shown in comparison with the expected decay-time distributions [35] for ^{258}Sg [36] and ^{259}Sg [36]. Details of the observed α-decay chains together with their negligibly low calculated random probabilities are given in Ref. [37]. Cross-section values deduced from these events shown in Fig. 1(a) differ from the ones reported in Ref. [27] but are in line with excitation functions calculated by the statistical code HIVAP [35], with the parameters describing the $^{54}Cr + ^{207,208}Pb$ reactions [41,42].

In Run 2, where two ^{206}Pb target segments were irradiated at $E_b = 252.4$ MeV, one ER–FI event with $\Delta t = 42$ ms was observed. This event was considered to originate from the $1n$ channel of the $^{52}Cr + ^{206}Pb$ reaction. Based on the cross section of this one event and the HIVAP results [see Fig. 1(b)], the beam energy was lowered to accumulate higher statistics and to measure the excitation function for the $1n$ channel. We observed further 21 and 1 ER–FI events with $\Delta t < 1$ s at $E_b = 251.6$ and 249.0 MeV, respectively. The total number of randomly correlated ER–FI events was calculated to be three. Individual Δt values of all ER–FI events, including the one from Run 2 are shown in Fig. 1(d). In addition, one ER–α(9.30 MeV) event with $\Delta t = 8$ ms was observed at $E_b = 251.6$ MeV. Based on its Δt being similar to those of the ER–FI sequences it was attributed to originate from the same nucleus. The time distribution of all these 24 (23 FI and 1 α) events [see Fig. 1(d)] was fitted with a decay-time distribution according to Ref. [35] and a half-life of 12.6-ms was deduced. According to the fit, the two ER–FI events with the longest Δt do not belong to the 12.6-ms activity; thus, they are assigned to be random events. This is in line with the above mentioned expected number of random events.

Figure 1(d) reveals one more noticeable deviation. Based on the total number of events (22) assigned to the 12.6-ms activity, 0.3 events with $\Delta t < 0.2$ ms are expected to be observed instead of the two. These two ER–FI events with Δt of 58.2 μs and 108.9 μs may originate from a different state in ^{257}Sg. An origin from hitherto unknown ^{256}Sg is unlikely because a negligibly low cross section for the $2n$ channel at $E_b = 251.6$ MeV is predicted by HIVAP [see Fig. 1(b)].

Alpha-decay branching of the 12.6-ms state, estimated as ≈0.1, results in a partial half-life (T_α) of ≈0.13 s.

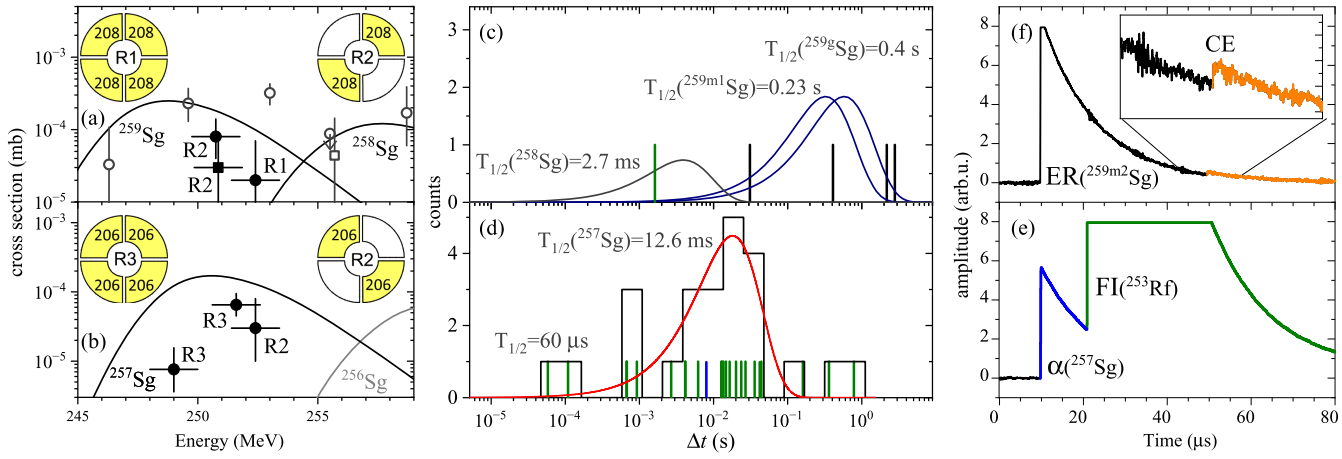


FIG. 1. The experimental and theoretical (HIVAP [43]) cross sections of the (a) ^{52}Cr + ^{208}Pb and (b) ^{52}Cr + ^{206}Pb reactions are shown by symbols and lines, respectively. The used target segments for Run 1 (R1), Run 2 (R2) and Run 3 (R3) are illustrated for each reaction. Circles and squares correspond to the experimental cross sections for the 1n and 2n channels, respectively. Open and solid symbols are the data from Ref. [27] and from this work, respectively. The cross-section values from Run 2 with two ^{208}Pb target segments shown in (a) are plotted at slightly shifted energies around the used beam energy of 250.8 MeV for better visibility. In (c), the correlation times (Δt) of one fission and four α events measured with ^{208}Pb and assigned to the decays of ^{258}Sg and ^{259}Sg are shown. In addition, expected time distributions ([35]) for the known decays of ^{258}Sg [36] and ^{259}Sg (^{259g}Sg: ground state and ^{259m1}Sg: isomeric state) [36] are shown. In (d), the time distribution of 23 fission events and one α event measured with ^{206}Pb is shown together with each individual Δt. The fitted decay-time distribution with a half-life of 12.6 ms attributed to the decay ^{257}Sg is shown. (e) X-strip trace of the α event with a following high-energy fission signal, which terminates the ER–α(^{257}Sg)–FI(^{253}Rf) chain. (f) X-strip trace of the ER event of the ER–α–FI chain assigned to ^{259}Sg. The implantation signal is followed by a low-energy signal, which was assigned to a conversion electron (CE) from the hitherto unknown isomeric state (^{259m2}Sg) in ^{259}Sg. See text for details.

This experimental value is in good agreement with $T_\alpha = 0.17^{+0.16}_{-0.06}$ s calculated for ^{257}Sg with the semiempirical formula from Refs. [44,45] by using the measured $E_\alpha = 9.30(7)$ MeV. Furthermore, the ER–α(9.30 MeV) sequence was terminated by a fission, which was detected in the trace of the α event. As seen in Fig. 1(e), a high-energy fission signal was recorded 11 μs after the α signal. Accordingly, this high-energy signal was attributed to the decay of the known 52.8-μs fissioning state in ^{253}Rf [8,9] and the observed ER–α–FI chain from the 12.6-ms state was unambiguously assigned to originate from ^{257}Sg. Thus, the fission events from the 12.6-ms state also originate from ^{257}Sg. Cross sections of these events shown in Fig. 1(b) are in agreement with the expected 1n excitation function of the ^{52}Cr + ^{206}Pb reaction.

The suggested decay scheme for ^{257}Sg is shown in Fig. 2. The $12.6^{+3.7}_{-2.3}$ ms activity was tentatively attributed to the $9/2^-[734]$ ground state in analogy to the well-established ground-state systematics for the lighter $N = 151$ isotones. For comparison, the decay scheme of ^{255}Rf [46–48] is also shown in Fig. 2. As seen in this isotone, two types of isomeric states (single-particle low-lying $5/2^+[622]$ and higher-lying high-K) decaying via electromagnetic transitions exist. However, based on experimental evidence [12,24] that direct fission from high-K isomeric states is strongly hindered, the 60-μs fission could originate from a low-lying $5/2^+[622]$ state. According to the well-established systematics for the lighter $N = 151$ isotones [49], the $5/2^+[622]$ states decay electromagnetically with half-lives in the order of tens of μs with a large internal-conversion branching. Therefore, we searched for conversion-electron (CE) signals in all ER traces assigned to ^{257}Sg, but none were found above the ≈30 keV noise level. Accordingly, we cannot prove the $5/2^+[622]$ nature for the 60-μs fission events and the assignment given in Fig. 2 is tentative. At the same time, the nonobservation of CE suggests that no high-K state in ^{257}Sg decaying within a time range of 1–80 μs was populated with a probability larger than 5%.

Eventually, K isomers with μs half-lives in Fm-Rf [14–18] are typically produced in fusion-evaporation reactions with significantly large (< 50%) population probabilities [29,51–55]. In this regard, we also inspected the ER traces of events assigned to decays of ^{258}Sg and ^{259}Sg for the presence of CEs. In one of the four ER traces of ^{259}Sg, a CE signal with an energy of 0.25 MeV was recorded 40 μs after the ER as shown in Fig. 1(f). We consider this ER–CE event as strong evidence for the presence of a high-K isomeric state in ^{259}Sg. The roughly estimated population probability is 25% (1/4).

Our result on the ground state of ^{257}Sg confirms that fission is a dominant decay mode in the heavy neutron-deficient nuclei. Nevertheless, fission hindrance induced by the high-spin $9/2^-[734]$ level enabled the α transition between ^{257}Sg and ^{253}Rf. The excitation energy of the $9/2^-[734]$ state in ^{253}Rf cannot be estimated with the evaluated atomic mass table [56] since the ground-state to ground-state Q_α value

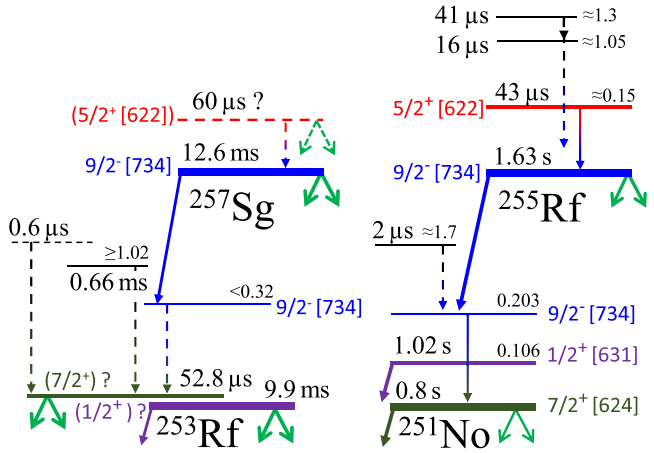


FIG. 2. Suggested decay schemes for ^{257}Sg and for the daughter ^{253}Rf [8,9] are shown in comparison with simplified ones for ^{255}Rf [46–48] and ^{251}No [50]. Single-particle levels, half-lives, and excitation energies (in MeV) are given. Levels and decays given by dashed lines and configurations in brackets have tentative assignments. Levels drawn with shorter lines mark the K-isomeric states. Data for ^{253}Rf were taken from the recent works [8,9].

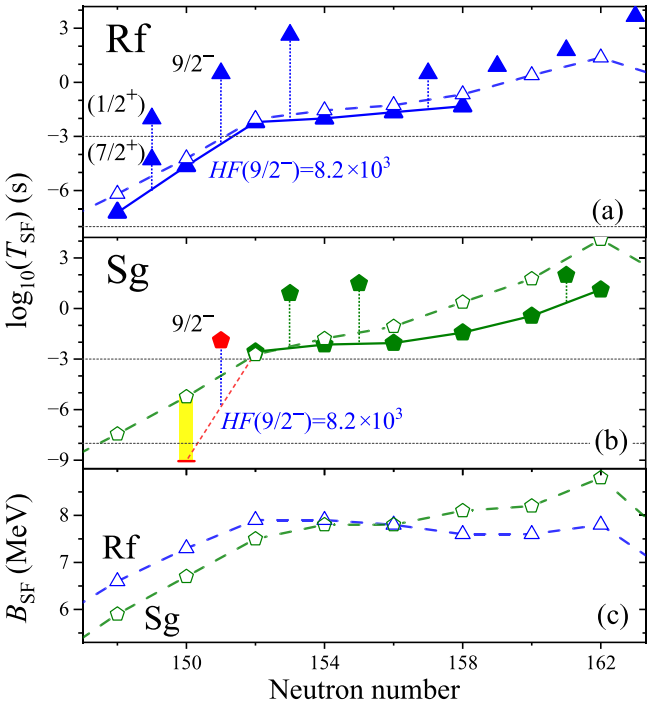


FIG. 3. The spontaneous fission half-lives of (a) Rf and (b) Sg isotopes are shown as a function of the neutron number. Horizontal dashed lines correspond to 1 ms and 10 ns. The experimental data are taken from Ref. [3], and even-even and even-odd nuclei are marked with solid and open symbols, respectively. The half-life for ^{252}Rf is taken from Ref. [18]. The presently measured value for ^{257}Sg is highlighted. Theoretical half-lives for the even-even Rf and Sg isotopes are from Ref. [66] and are given by dashed lines in (a) and (b). The corresponding dynamical fission-barrier heights for Rf and Sg [66] are shown in (c). In the case of odd-A nuclei, the vertical dotted line indicates the fission hindrance relative to the geometric mean of the half-lives of the two neighboring even-even nuclei [4,5]. A hindrance factor (HF) for ^{255}Rf and spin parities of states relevant to the discussion are given. The expected half-life range for the hitherto unknown ^{256}Sg is marked by the shaded region. See text for details.

for ^{257}Sg is not tabulated. The theoretically predicted Q_α values largely deviate from model to model and are sensitive to the nuclear masses calculated with a shell effect at $N = 152$ [57–61].

In the $N = 149$ isotones (^{251}No, ^{245}Cm, and ^{243}Pu [50,62–65], $9/2^-[734]$ excited states are feeding into the $7/2^+[624]$ ground state, bypassing the $1/2^+[631]$ state (see Fig. 2). Based on this, the 11-μs fission following the α decay of ^{257}Sg likely originates from the $7/2^+[624]$ state in ^{253}Rf. This agrees with results from Ref. [9], where the 52.8-μs fissioning state was populated in the deexcitation of a high-K isomeric state and, thus, was assigned to have a $7/2^+[624]$ configuration. Actually, this 52.8-μs state has also been observed to be populated in the decay of another tentatively assigned 0.6-μs isomeric state in ^{253}Rf [8]. A similarly short-lived K isomer decaying predominantly into the $9/2^-[734]$ state, which in turn deexcites into the ground-state band is known in the lighter ^{251}No isotone (see Fig. 2) [50]. Finally, all these findings on fission from ^{253}Rf support the decay scheme proposed in Ref. [9], where a high-K state is more fissile than a low-K state, which contradicts the systematics as known to date [3,4]. However, prior to drawing a final conclusion, decay patterns of two high-K isomeric states, of the $9/2^-[734]$ state and lower-lying states in ^{253}Rf have to be established.

In Figs. 3(a) and 3(b), currently known experimental T_{SF} for Rf and Sg isotopes are shown together with the theoretical values from Ref. [66]. The fission half-lives of both known states in ^{253}Rf are longer than the "unhindered" T_{SF} defined as a geometric mean of two half-lives of the neighboring even-even nuclei [4,5]. In this regard, the fission from the $9/2^-$ ground state of ^{257}Sg is certainly hindered as $T_{SF}(^{257}\text{Sg})$ is longer than $T_{SF}(^{258}\text{Sg})$ and towards the hitherto unknown ^{256}Sg, a decrease in T_{SF} by a factor of about 3×10^2 (relative to ^{258}Sg) is anticipated according to the theory as seen in Fig. 3(b). By taking the theoretically predicted $T_{SF}(^{256}\text{Sg}) = 6$ μs one can estimate a hindrance factor of HF $\approx 10^2$. On the other hand, the same state known in the lighter ^{255}Rf isotone has a larger HF $= 8.2 \times 10^3$ [3]. Apparently, by taking this larger HF for ^{257}Sg, one can roughly estimate a lower limit for $T_{SF}(^{256}\text{Sg}) \approx 1$ ns, which is more than 3 orders of magnitude shorter than the theoretically predicted value of 6 μs. This could indicate that a sudden fall in T_{SF} of ^{256}Sg compared to theory is not excluded.

In general, theoretical predictions from Ref. [66] describe quite well the plateaulike T_{SF} trends in both Rf

and Sg with $N \geq 152$ but with noticeable deviations for Sg towards $N = 162$. In Fig. 3(c), heights of fission barriers are shown, which account for fission dynamics on the potential energy surface, from which the theoretical T_{SF} were calculated. These correspond to the single-humped barriers since the outer barrier of superheavy nuclei is commonly agreed to disappear in the region of $Z = 104$–108 [66–70]. As seen, the overestimated half-lives of Sg isotopes around $N = 162$ are mainly due to larger calculated fission-barrier heights. In the region of neutron-deficient nuclei, theory predicts Sg to have lower fission barriers compared to the Rf isotones, which result in shorter half-lives [cf. Figs. 3(a) and 3(b)]. Thus, if a sudden fall in the T_{SF} of ^{256}Sg occurs relative to the theory then it has to be associated with a significant reduction in the calculated fission-barrier height for ^{256}Sg. On the other hand, the recent analysis of the fission-barrier widths carried out in Ref. [71] showed that the outer fission barrier may appear back in cases of the even-even $^{258–266}$Sg isotopes. If this will be the case then one can expect a sudden decrease in the T_{SF}-trend in the even-even neutron-deficient Sg isotopes with $N < 152$ caused by the transition of the fission-barrier shape from double humped to single humped. Nevertheless, these discussions show the necessity for the expansion of the experimental T_{SF} systematics of Sg isotopes, i.e., for the synthesis of ^{256}Sg, for which a half-life in the range of 1 ns − 6 μs is to be expected.

In this Letter, we present the results on neutron-deficient Sg isotopes produced in the $^{52}\mathrm{Cr} + {}^{206,208}\mathrm{Pb}$ fusion-evaporation reactions. We discovered the new isotope ^{257}Sg, which decays by spontaneous fission and α-particle emission with a half-life of $12.6^{+3.7}_{-2.3}$ ms. The observed α decay, attributed to originate from the $9/2^-$ ground state, populates a state in ^{253}Rf, which underwent fission after 11 μs. This supports the recent observation reported in Ref. [9], which led to the assignment of a 58-μs fission to originate from a high-spin $7/2^+$ state. More detailed experimental data on ^{253}Rf are necessary for the final verification of the above assignment. In addition, we observed strong evidence for the occurrence of a K-isomeric state in ^{259}Sg. The fission half-life of ^{257}Sg, discussed within the systematics of the fission hindrance caused by the K-quantum number led to the conclusion of a possible sudden fall (down to ≈1 ns) in the fission half-life of the hitherto unknown ^{256}Sg, for which theory predicts 6 μs. Such a scenario would represent a hitherto unseen feature in the fission-landscape of superheavy nuclei highlighting the need for further exploration of the fission phenomena.

Acknowledgments—We are grateful to GSI's ion-source and UNILAC staff, the Experiment Electronics, and the Target Laboratory departments for their support of the experiment. This work was supported by the German BMBF (Grant No. 05P21UMFN2). The publication is funded by the Open Access Publishing Fund of GSI Helmholtzzentrum für Schwerionenforschung. The results presented here are based on the experiment G-22-00034, which was performed at the beam line X8/TASCA at the GSI Helmholtzzentrum für Schwerionenforschung, Darmstadt (Germany) in the frame of FAIR Phase-0.

Data availability—The data supporting this study's findings are available within the article.

[1] Yu. Ts. Oganessian, A. Sobiczewski, and G. M. Ter-Akopian, Phys. Scr. **92**, 023003 (2017).
[2] S. Hofmann and G. Münzenberg, Rev. Mod. Phys. **72**, 733 (2000).
[3] F. P. Heßberger, Eur. Phys. J. A **53**, 75 (2017).
[4] D. C. Hoffman, Nucl. Phys. **A502**, 21 (1989).
[5] J. Randrup, C. Tsang, P. Möller, S. Nilsson, and S. Larsson, Nucl. Phys. **A217**, 221 (1973).
[6] S. Ćwiok, S. Hofmann, and W. Nazarewicz, Nucl. Phys. **A573**, 356 (1994).
[7] O. R. Smits, Ch. E. Düllmann, P. Indelicato, W. Nazarewicz, and P. Schwerdtfeger, Nat. Rev. Phys. **6**, 86 (2024).
[8] J. Khuyagbaatar, H. Brand, R. A. Cantemir, Ch. E. Düllmann, F. P. Heßberger, E. Jäger, B. Kindler, J. Krier, N. Kurz, B. Lommel, B. Schausten, and A. Yakushev, Phys. Rev. C **104**, L031303 (2021).
[9] A. Lopez-Martens *et al.*, Phys. Rev. C **105**, L021306 (2022).
[10] J. L. Pore, W. Younes, J. M. Gates, L. M. Robledo, F. H. Garcia, R. Orford, H. L. Crawford, P. Fallon, J. A. Gooding, M. Kireeff Covo, M. McCarthy, and M. A. Stoyer, Phys. Rev. C **110**, L041301 (2024).
[11] J. Khuyagbaatar *et al.*, Phys. Rev. Lett. **125**, 142504 (2020).
[12] A. Lopez-Martens *et al.*, EPJ Web Conf. **290**, 02027 (2023).
[13] I. S. Rogov, G. G. Adamian, and N. V. Antonenko, Phys. Rev. C **110**, 014606 (2024).
[14] F. Kondev, G. Dracoulis, and T. Kibédi, At. Data Nucl. Data Tables **103–104**, 50 (2015).
[15] P. M. Walker and F. G. Kondev, Eur. Phys. J. Special Topics **233**, 983 (2024).
[16] D. Ackermann, S. Antalic, and F. P. Heßberger, Eur. Phys. J. Special Topics **233**, 1017 (2024).
[17] K. Kessaci, B. J. P. Gall, O. Dorvaux, M. Forge, A. Lopez-Martens, R. Chakma, K. Hauschild, M. L. Chelnokov, V. I. Chepigin, A. V. Isaev, A. A. Kuznetsova, O. N. Malyshev, R. Mukhin, J. Piot, A. G. Popeko, Y. A. Popov, E. A. Sokol, A. I. Svirikhin, and A. V. Yeremin, Phys. Rev. C **110**, 054310 (2024).
[18] J. Khuyagbaatar, P. Mosat, J. Ballof, R. A. Cantemir, Ch. E. Düllmann, K. Hermainski, F. P. Heßberger, E. Jäger, B. Kindler, J. Krier, N. Kurz, S. Löchner, B. Lommel, B. Schausten, Y. Wei, P. Wieczorek, and A. Yakushev, Phys. Rev. Lett. **134**, 022501 (2025).
[19] F. R. Xu, E. G. Zhao, R. Wyss, and P. M. Walker, Phys. Rev. Lett. **92**, 252501 (2004).
[20] R.-D. Herzberg *et al.*, Nature (London) **442**, 896 (2006).
[21] G. G. Adamian, N. V. Antonenko, and W. Scheid, Phys. Rev. C **81**, 024320 (2010).
[22] P. M. Walker, F. R. Xu, H. L. Liu, and Y. Sun, J. Phys. G **39**, 105106 (2012).
[23] P. M. Walker and F. R. Xu, Phys. Scr. **91**, 013010 (2016).

[24] J. Khuyagbaatar, Eur. Phys. J. A **58**, 243 (2022).
[25] A. Semchenkov, W. Brüchle, E. Jäger, E. Schimpf, M. Schädel, C. Mühle, F. Klos, A. Türler, A. Yakushev, A. Belov, T. Belyakova, M. Kaparkova, V. Kukhtin, E. Lamzin, and S. Sytchevsky, Nucl. Instrum. Methods Phys. Res., Sect. B **266**, 4153 (2008).
[26] E. Jäger, H. Brand, Ch. E. Düllmann, J. Khuyagbaatar, J. Krier, M. Schädel, T. Torres, and A. Yakushev, J. Radioanal. Nucl. Chem. **299**, 1073 (2014).
[27] C. M. Folden III, I. Dragojević, Ch. E. Düllmann, R. Eichler, M. A. Garcia, J. M. Gates, S. L. Nelson, R. Sudowe, K. E. Gregorich, D. C. Hoffman, and H. Nitsche, Phys. Rev. C **79**, 027602 (2009).
[28] J. Khuyagbaatar *et al.*, Nucl. Instrum. Methods Phys. Res., Sect. A **689**, 40 (2012).
[29] J. Khuyagbaatar *et al.*, Nucl. Phys. **A994**, 121662 (2020).
[30] K. E. Gregorich, Nucl. Instrum. Methods Phys. Res., Sect. A **711**, 47 (2013).
[31] J. Khuyagbaatar, V. P. Shevelko, A. Borschevsky, Ch. E. Düllmann, I. Y. Tolstikhina, and A. Yakushev, Phys. Rev. A **88**, 042703 (2013).
[32] N. Kurz, J. Hoffmann, S. Minami, and W. Ott, GSI Report 2012-1, 2012, p. 252.
[33] https://www.gsi.de/work/forschung/experimentelektronik
[34] J. Khuyagbaatar, H. Brand, Ch. E. Düllmann, F. P. Heßberger, E. Jäger, B. Kindler, J. Krier, N. Kurz, B. Lommel, Y. Nechiporenko, Y. N. Novikov, B. Schausten, and A. Yakushev, Phys. Rev. C **106**, 024309 (2022).
[35] K. H. Schmidt, C. C. Sahm, K. Pielenz, and H. G. Clerc, Z. Phys. A **316**, 19 (1984).
[36] F. Kondev, M. Wang, W. Huang, S. Naimi, and G. Audi, Chin. Phys. C **45**, 030001 (2021).
[37] See Supplemental Material at http://link.aps.org/supplemental/10.1103/s7hr-y7zq for details of all observed alpha-decay chains, which includes Refs. [38–40].
[38] F. P. Heßberger, S. Hofmann, V. Ninov, P. Armbruster, H. Folger, G. Münzenberg, H. J. Schött, A. G. Popeko, A. V. Yeremin, A. N. Andreyev, and S. Saro, Z. Phys. A **359**, 415 (1997).
[39] A. I. Svirikhin *et al.*, Phys. Part. Nucl. Lett. **18**, 445 (2021).
[40] M. S. Tezekbayeva *et al.*, Eur. Phys. J. A **58**, 52 (2022).
[41] B. Sulignano, Search for K isomers in ^{252,254}No and ^{260}Sg and investigation of their nuclear structure, Ph.D. thesis, Johannes Gutenberg-Universität Mainz, Germany, 2007.
[42] B. Streicher, F. P. Heßberger, S. Antalic, S. Hofmann, D. Ackermann, S. Heinz, B. Kindler, J. Khuyagbaatar, I. Kojouharov, P. Kuusiniemi, M. Leino, B. Lommel, R. Mann, Š. Šáro, B. Sulignano, J. Uusitalo, and M. Venhart, Eur. Phys. J. A **45**, 275 (2010).
[43] W. Reisdorf, Z. Phys. A **300**, 227 (1981).
[44] D. Poenaru, M. Ivascu, and D. Mazilu, J. Phys. Lett. **41**, 589 (1980).
[45] E. Rurarz, Acta Phys. Pol. B **14**, 917 (1983), https://www.actaphys.uj.edu.pl/R/14/12/917.
[46] S. Antalic, F. P. Heßberger, D. Ackermann, S. Heinz, S. Hofmann, B. Kindler, J. Khuyagbaatar, B. Lommel, and R. Mann, Eur. Phys. J. A **51**, 41 (2015).
[47] P. Mosat *et al.*, Phys. Rev. C **101**, 034310 (2020).
[48] R. Chakma, A. Lopez-Martens, K. Hauschild, A. V. Yeremin, O. N. Malyshev, A. G. Popeko, Y. A. Popov, A. I. Svirikhin, V. I. Chepigin, E. A. Sokol, A. V. Isaev, A. A. Kuznetsova, M. L. Chelnokov, M. S. Tezekbayeva, I. N. Izosimov, O. Dorvaux, B. Gall, and Z. Asfari, Phys. Rev. C **107**, 014326 (2023).
[49] M. Asai, F. P. Heßberger, and A. Lopez-Martens, Nucl. Phys. **A944**, 308 (2015).
[50] F. P. Heßberger, S. Hofmann, D. Ackermann, S. Antalic, B. Kindler, I. Kojouharov, P. Kuusiniemi, M. Leino, B. Lommel, R. Mann, K. Nishio, A. G. Popeko, B. Sulignano, S. Saro, B. Streicher, M. Venhart, and A. V. Yeremin, Eur. Phys. J. A **30**, 561 (2006).
[51] B. Sulignano, S. Heinz, F. P. Heßberger, S. Hofmann, D. Ackermann, S. Antalic, B. Kindler, I. Kojouharov, P. Kuusiniemi, B. Lommel, R. Mann, K. Nishio, A. G. Popeko, S. Saro, B. Streicher, M. Venhart, and A. V. Yeremin, Eur. Phys. J. A **33**, 327 (2007).
[52] F. P. Heßberger *et al.*, Eur. Phys. J. A **43**, 55 (2010).
[53] H. M. David *et al.*, Phys. Rev. Lett. **115**, 132502 (2015).
[54] J. Kallunkathariyil *et al.*, Phys. Rev. C **101**, 011301(R) (2020).
[55] J. Khuyagbaatar, H. Brand, R. A. Cantemir, Ch. E. Düllmann, M. Götz, S. Götz, F. P. Heßberger, E. Jäger, B. Kindler, J. Krier, N. Kurz, B. Lommel, B. Schausten, and A. Yakushev, Phys. Rev. C **103**, 064303 (2021).
[56] M. Wang, W. Huang, F. Kondev, G. Audi, and S. Naimi, Chin. Phys. C **45**, 030003 (2021).
[57] A. Wapstra and K. Bos, At. Data Nucl. Data Tables **17**, 474 (1976).
[58] Y. Aboussir, J. Pearson, A. Dutta, and F. Tondeur, At. Data Nucl. Data Tables **61**, 127 (1995).
[59] H. Koura, T. Tachibana, M. Uno, and M. Yamada, Prog. Theor. Phys. **113**, 305 (2005).
[60] N. Wang, M. Liu, X. Wu, and J. Meng, Phys. Lett. B **734**, 215 (2014).
[61] P. Möller, A. Sierk, T. Ichikawa, and H. Sagawa, At. Data Nucl. Data Tables **109–110**, 1 (2016).
[62] S. W. Yates, I. Ahmad, A. M. Friedman, F. J. Lynch, and R. E. Holland, Phys. Rev. C **11**, 599 (1975).
[63] I. Ahmad, J. P. Greene, F. G. Kondev, and S. Zhu, Phys. Rev. C **91**, 044310 (2015).
[64] P. Fields, I. Ahmad, A. Friedman, J. Lerner, and D. Metta, Nucl. Phys. **A160**, 460 (1971).
[65] F. P. Heßberger, S. Hofmann, D. Ackermann, P. Cagarda, R.-D. Herzberg, I. Kojouharov, P. Kuusiniemi, M. Leino, and R. Mann, Eur. Phys. J. A **22**, 417 (2004).
[66] R. Smolańczuk, J. Skalski, and A. Sobiczewski, Phys. Rev. C **52**, 1871 (1995).
[67] S. G. Nilsson, C. F. Tsang, A. Sobiczewski, Z. Szymański, S. Wycech, C. Gustafson, I.-L. Lamm, P. Möller, and B. Nilsson, Nucl. Phys. **A131**, 1 (1969).
[68] Y. Oganessian, A. G. Demin, A. S. Iljinov, S. P. Tretyakova, A. A. Pleve, Yu. E. Penionzhkevich, M. P. Ivanov, and Yu. P. Tretyakov, Nucl. Phys. **A239**, 157 (1975).
[69] F. Heßberger, G. Münzenberg, S. Hofmann, P. Armbruster, Y. Agarwal, W. Reisdorf, K. Poppensieker, K.-H. Schmidt, J. Schneider, W. Schneider, H. Schött, C.-C. Sahm, D. Vermeulen, and B. Thuma, J. Less-Common Met. **122**, 445 (1986).
[70] R. Smolańczuk, Phys. Rev. C **56**, 812 (1997).
[71] J. Khuyagbaatar, Nucl. Phys. **A1002**, 121958 (2020).